Int. J. Heat Mass Transfer. Vol. 35, No. 11, pp. 3105–3113, 1992
Printed in Great Britain

0017–9310/92 $5.00 + 0.00

Conjugate free convection from a circular cylinder in a porous medium

SHIGEO KIMURA
Government Industrial Research Institute, Tohoku Nigatake 4-2-1, Miyagino, Sendai 983, Japan

and

IOAN POP
University of Cluj, Faculty of Mathematics, R-3400 Cluj, CP253, Romania

(*Received* 19 *September* 1991 *and in final form* 13 *November* 1991)

Abstract—The purpose of this paper is to formulate and solve the problem of steady free convection from a horizontal circular cylinder with a heated core embedded in a fluid-saturated porous medium. The governing equations were solved numerically using an efficient finite-difference technique. The effects of various parameters entering in the problem are presented in tabular and graphical forms. The thermal conductivity ratios of the cylinder wall to the porous medium vary from 0.5 to infinity. The ratio of cylinder inner radius to outer radius was 0.2, 0.5 and 0.9. The results were compared with the exact solution for the extreme case of a non-conjugate problem. Approximate solutions for the average boundary temperature between cylinder and porous matrix and for the average Nusselt number are also found, and the results are confirmed by numerical computations. It may be remarked that the present analysis gives compact formulae to provide useful information on the temperature distribution and the heat transfer from a cylinder and may find wide applications in the field of various thermal technologies.

1. INTRODUCTION

THE PROBLEM of free and forced convection from a horizontal heated cylinder embedded in a fluid-saturated porous medium is of considerable practical and fundamental interest. This occurs in a number of practical applications such as oil recovery techniques (steam flooding process), in biomechanical problems (blood flow in the pulmonary alveolar sheet), in filtration, transpiration cooling, heat pipe technology and geothermal energy recovery and so there is a large amount of literature on the subject. The survey articles by Cheng [1] and Bejan [2], summarize very well the work done on this problem. Apart from these review articles it is, however, worth mentioning that free convection flows from horizontal cylinders have been investigated theoretically by many researchers such as Fernandez and Schrock [3], Merkin [4], Nilson [5], Ingham *et al.* [6], Hasan and Mujumdar [7], Ingham and Pop [8], Nakayama and Koyama [9], and Farouk and Shayer [10]. Experimental work has also been carried out by several researchers, see for instance, the papers by Schrock *et al.* [11] and Fand *et al.* [12]. The flow and temperature distributions in the forced convection circumstance have been studied by Sano [13], Ingham and Pop [14], Vasantha *et al.* [15], Kimura [16–18], and Pop and Cheng [19].

In many problems of practical interest, however, convection heat transfer depends strongly on the thermal boundary conditions. Free convection must then be studied as a mixed problem, which is termed a conjugate problem. The phenomenon depends on several parameters showing that in many cases this strong dependence does exist.

Conjugate free convection flows about a circular cylinder immersed in a saturated porous medium have received little attention so far. Successful analytical solutions have, however, been obtained for problems of conjugate free convection flows about a tapered downward projecting fin of a simple power law form in a porous medium, see for example, papers by Pop *et al.* [20, 21], Liu *et al.* [22, 23], and Nakayama and Koyama [24], among others.

In this paper, we consider the problem of conjugate free convection about a horizontal circular cylinder of thermal conductivity k_s, which is placed in a fluid-saturated porous medium of thermal conductivity k_f and a constant temperature T_∞. It is assumed that the cylinder has a heated core region of a uniform temperature T_c, where $T_c > T_\infty$. Heat moves through the cylinder by two-dimensional conduction and is transferred from the solid–porous matrix interface by laminar free convection to the ambient fluid–porous medium.

The purpose of the present paper is, therefore, to predict theoretically the flow and temperature distributions in the fluid–porous medium region by the common solution of the momentum and energy equations for the solid and the fluid, respectively. Of special importance is the temperature distribution at the

NOMENCLATURE

a	radius of the cylinder
a_c	radius of the core region
A	a finite distance from a cylinder center
g	acceleration due to gravity
k	thermal conductivity ratio, k_s/k_f
k_f	effective thermal conductivity of the porous medium
k_s	conductivity of cylinder wall
K	permeability of the porous medium
M	a total number of grid points in the radial direction
N	a total number of grid points in the angular direction
Nu	local Nusselt number, $-(a/\Delta T)(\partial T_f/\partial r')_{r'=a}$
$\overline{Nu}$	average Nusselt number, $\int_0^\pi Nu\, d\phi/\pi$
q''	heat flux per unit area
$\overline{q''}$	average heat flux per unit area
r	dimensionless radial coordinate
R	radius ratio, a_c/a
Ra	Rayleigh number for the porous medium, $Kg\beta(T_c-T_\infty)a/\alpha\nu$
T	temperature
T_f	temperature in the convecting fluid
T_s	temperature in the solid cylinder
$\overline{T}_b$	dimensionless average boundary temperature, $(T_b-T_\infty)/(T_c-T_\infty)$
T_c, T_∞	temperatures (constant) of the core region and ambient fluid, respectively
ΔT	applied temperature difference, T_c-T_∞
u, v	dimensionless velocity components along (r, ϕ) axes.

Greek symbols

α	thermal diffusivity
β	coefficient of thermal expansion
δ	boundary layer thickness
$\Delta\theta$	temperature increment
$\Delta\psi$	streamline increment
θ	dimensionless temperature
λ	constant, equation (24)
ν	kinematic viscosity
ϕ	angular coordinate
ψ	dimensionless stream function.

Subscripts

f	variables in the fluid–porous medium
s	variables in the solid
i, j	nodal points.

Superscripts

$'$	dimensional variables
$\overline{\ }$	average quantities
n	iteration order.

interface between the solid cylinder and porous matrix and the overall transfer coefficients from the heated core to the ambient porous medium. Numerical solutions of the full momentum and energy equations are generated by using a finite-difference method. In addition, simple approximate analytical solutions for the average boundary temperature between solid and porous matrix and the average Nusselt number were derived when the Rayleigh number is large ($Ra \gg 1$), i.e. boundary layer approximation. Such analytical solutions have apparently not been presented before and have an advantage over the numerical results from a practical point of view. The results given by these formulae are consistent with the carefully performed numerical solutions.

It may be mentioned to this end that important contributions to the problem of conjugate heat transfer from circular cylinders in low Reynolds number Newtonian fluids were made by Sundén [25, 26].

2. GOVERNING EQUATIONS

Consider the steady free convection flow from a circular cylinder of radius a embedded in a fluid-saturated porous medium of a uniform temperature T_∞. The cylinder has a heated core region of radius a_c, with $a_c < a$, where $T_c > T_\infty$. The geometry and the coordinate system are shown in Fig. 1. If we make use of the polar system of coordinates (r', ϕ) and assume that the angular coordinate is measured clockwise from the vertically down position and that the problem is symmetric about a vertical plane passing through the axis of the cylinder, then consideration will be confined to the range $0 < \phi < \pi$ (or $\pi < \phi < 2\pi$). We also assume that the porous material is isotropic and homogeneous, and the fluid is incom-

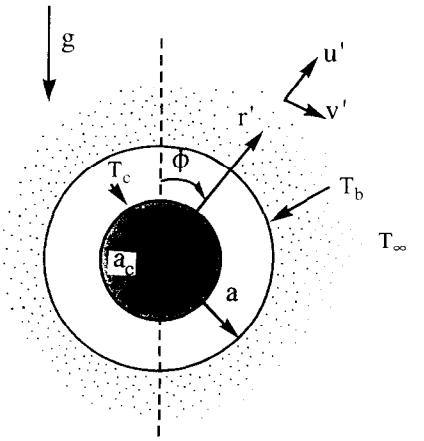

FIG. 1. Physical model and coordinate system.

pressible. Under these assumptions and invoking the Boussinesq–Darcy approximation, the free convection flow from the solid cylinder is described by the equations of continuity

$$\frac{\partial}{\partial r'}(r'u')+\frac{\partial v'}{\partial \phi}=0 \tag{1}$$

and momentum

$$\frac{1}{r'}\frac{\partial u'}{\partial \phi}-\frac{v'}{r'}-\frac{\partial v'}{\partial r'}=\frac{g\beta K}{\nu}\left(\frac{\partial T_f}{\partial r'}\sin\phi+\frac{\partial T_f}{\partial \phi}\frac{\cos\phi}{r'}\right) \tag{2}$$

equation of energy in the fluid–porous medium

$$u'\frac{\partial T_f}{\partial r'}+\frac{v'}{r'}\frac{\partial T_f}{\partial \phi}=\alpha\left[\frac{1}{r'}\frac{\partial}{\partial r'}\left(r'\frac{\partial T_f}{\partial r'}\right)+\frac{1}{r'^2}\frac{\partial^2 T_f}{\partial \phi^2}\right] \tag{3}$$

equation of heat transfer inside the cylinder

$$\frac{\partial}{\partial r'}\left(r'\frac{\partial T_s}{\partial r'}\right)+\frac{1}{r'^2}\frac{\partial^2 T_s}{\partial \phi^2}=0 \tag{4}$$

where (u', v') are the velocity components in the r' and ϕ directions, and T_f and T_s are the temperatures of the fluid-saturated porous medium and of the solid cylinder, respectively. Equations (1) to (4) are to be solved with respect to the following boundary conditions at the fluid–wall interface

$$u'=0,\quad T_f=T_s,\quad k_f\frac{\partial T_s}{\partial r'}=k_s\frac{\partial T_s}{\partial r'}\quad \text{at}\quad r'=a \tag{5}$$

within the core region

$$T_s=T_c\quad \text{at}\quad r'=a_c \tag{6}$$

far away from the cylinder

$$u'=v'=0,\quad T_f=T_\infty\quad \text{as}\quad r'\to\infty \tag{7}$$

symmetry conditions

$$\psi'=\frac{\partial T_f}{\partial \phi}=\frac{\partial T_s}{\partial \phi}=0\quad \text{along}\quad \phi=0,\pi. \tag{8}$$

The governing system of equations (1) to (4) was first transformed into a dimensionless form before it was solved numerically. To achieve this, one introduces the following dimensionless variables

$$r=r'/a,\quad \psi=\psi'/\alpha,\quad u=au'/\alpha,\quad v=av'/\alpha$$
$$\theta=(T-T_\infty)/\Delta T,\quad R=a_c/a,\quad k=k_s/k_f \tag{9}$$

where $\Delta T=T_c-T_\infty$ and ψ' is the stream function satisfying the continuity equation with

$$u'=\frac{1}{r'}\frac{\partial \psi'}{\partial \phi},\quad v'=-\frac{\partial \psi'}{\partial r'}. \tag{10}$$

By introducing equation (9) into equations (2)–(4), we arrive at the following dimensionless system of equations

$$\nabla^2\psi=Ra\left(\frac{\partial \theta_f}{\partial r}\sin\phi+\frac{\partial \theta_f}{\partial \phi}\frac{\cos\phi}{r}\right) \tag{11}$$

$$u\frac{\partial \theta_f}{\partial r}+\frac{v}{r}\frac{\partial \theta_f}{\partial \phi}=\nabla^2\theta_f \tag{12}$$

$$\nabla^2\theta_s=0 \tag{13}$$

subject to the boundary conditions

$$\psi=0,\quad \theta_f=\theta_s,\quad \frac{\partial \theta_f}{\partial r}=k\frac{\partial \theta_s}{\partial r}\quad \text{at}\quad r=1 \tag{14}$$

$$\theta_s=1\quad \text{at}\quad r=R \tag{15}$$

$$\psi=0,\quad \theta_f=0\quad \text{as}\quad r\to\infty \tag{16}$$

$$\psi=\frac{\partial \theta_f}{\partial \phi}=\frac{\partial \theta_s}{\partial \phi}=0\quad \text{on}\quad \phi=0,\pi \tag{17}$$

where $Ra=g\beta\Delta TKa/\alpha\nu$ is the Rayleigh number for the fluid–porous medium and ∇^2 denotes the two-dimensional Laplacian.

The physical quantities of primary interest in this problem include the local and average Nusselt numbers, which are defined through the relations

$$Nu=-\frac{a}{\Delta T}\left(\frac{\partial T_f}{\partial r'}\right)_{r'=a},\quad \overline{Nu}=\frac{1}{\pi}\int_0^\pi Nu\,d\phi. \tag{18}$$

Using the non-dimensional variables (9), the heat transfer parameters can be written as

$$Nu=-\left(\frac{\partial \theta_f}{\partial r}\right)_{r=1},\quad \overline{Nu}=\frac{1}{\pi}\int_0^\pi\left(-\frac{\partial \theta_f}{\partial r}\right)_{r=1}d\phi. \tag{19}$$

3. APPROXIMATE ANALYTICAL SOLUTION

The coupled character of boundary conditions (14)–(17) preclude an analytical solution for the problem composed of equations (11)–(13). There is, however, a limiting condition, given by the boundary layer assumption that $Ra\gg 1$, valid in the region near the solid cylinder, where this problem possesses an analytical solution. It is logical, and as we shall see, quite fruitful, to attempt to report an analytical solution of the posed problem for this limiting case. In the interest of brevity, only the key formulae are reported.

From the one-dimensional equation of heat balance between the solid and fluid interface (at $r'=a$), the heat flux (per unit area) q'' can be expressed as

$$q''=\frac{2\pi k_s(T_c-T_b)}{2\pi a\ln(a/a_c)}=k_f\frac{T_b-T_\infty}{\delta} \tag{20}$$

where T_b is the average temperature at the surface of the cylinder defined by $\int_0^\pi T'(a,\phi)\,d\phi/\pi$, and δ is the thickness of the boundary layer along the cylinder, which, under the boundary layer approximation, is given by, see Ingham and Pop [8],

$$\delta/a=2.503Ra^{-1/2} \tag{21}$$

where Ra is the Rayleigh number defined by an effec-

tive temperature difference across a porous medium, and assumed to be much greater than unity. Consequently, equations (20) and (21) lead to the following approximate solution for the average boundary temperature between solid cylinder and porous matrix

$$\bar{T}_b = \frac{2.5k}{2.5k + Ra^{1/2} \ln (a/a_c)} \tag{22}$$

where $\bar{T}_b = (T_b - T_\infty)/(T_c - T_\infty)$, $k = k_s/k_f$. When k is large, the Rayleigh number based on temperature difference of $T_b - T_\infty$ is effectively the same as one based on $T_c - T_\infty$. On the contrary when k is small, the effective Ra based on $T_b - T_\infty$ is also small. In this case the temperature drop takes place mostly within the cylinder wall, and convection plays only a minor role in determining the boundary temperature. It can, therefore, be conceivable that equation (22) is relatively insensitive to the definition of the Rayleigh number; the Rayleigh number in equation (22) can be replaced by the *a priori* known Rayleigh number, which is based on the temperature difference $T_c - T_\infty$.

Further, from the definition of the average Nusselt number in terms of the non-dimensionalized T_b, we have

$$\overline{Nu} = \frac{\bar{q}''a}{k_f \Delta T} \sim \frac{T_b - T_\infty}{\Delta T} Ra^{1/2} \sim \bar{T}_b \, Ra^{1/2} \tag{23}$$

if equation (20) is used. Equation (23) suggests that the ratio of $\overline{Nu}$ to $\bar{T}_b \, Ra^{1/2}$ is always constant, that is

$$\frac{\overline{Nu}}{\bar{T}_b \, Ra^{1/2}} = \lambda \tag{24}$$

where λ is a constant to be found. Upon substituting equation (22) into equation (24), we finally obtain

$$\overline{Nu} = \frac{\lambda \, Ra^{1/2}}{1 + Ra^{1/2} \ln (a/a_c)/(2.5k)} \tag{25}$$

which may readily be evaluated once the unknown constant λ has been determined. Regarding the Rayleigh number the same argument as one given to equation (22) holds for equations (23)–(25). The validity of equations (24) and (25) will be tested extensively for various parametric values solving equations (11)–(13) with the boundary conditions (14)–(17) numerically in the next two sections. A value of λ of 0.4 was thus found to predict $\overline{Nu}$ with the help of equation (25).

The engineering significance of the results described by equations (22) and (25) is that $\bar{T}_b$ and $\overline{Nu}$ can be evaluated immediately, provided k $(=k_s/k_f)$, R $(=a_c/a)$ and Ra are specified.

Table 1. Effect of the size of computational domain on the average Nusselt number ($k \to \infty$)

Ra	Ingham and Pop [8]	Numerical			
		$A = 3$	$A = 5$	$A = 10$	$A = 15$
20	2.183	1.9227	2.0925	2.1492	2.1631
40	3.008	2.8683	2.9414	3.0299	3.0427
100	4.582	4.4474	4.5591	4.5882	4.6023
400	8.691	8.5981	8.7922	8.8290	8.8444

Table 2. Effect of a number of grid points on the average Nusselt number ($A = 10$, $k \to \infty$)

Ra	40×31	50×41
20	2.1261	2.1424
40	2.9714	2.9836
100	4.5882	4.5987
400	8.8290	8.8325

4. THE NUMERICAL COMPUTATIONS

Since the numerical scheme to be described in this section is quite similar to that employed in two recent papers by Kimura and Pop [27, 28] only an outline of this method will be presented here.

One difficulty in the present problem, particularly in a numerical point of view, is to determine appropriate far field boundary conditions. A possible condition would be an open boundary condition at a finite distance from a cylinder. The boundary conditions of

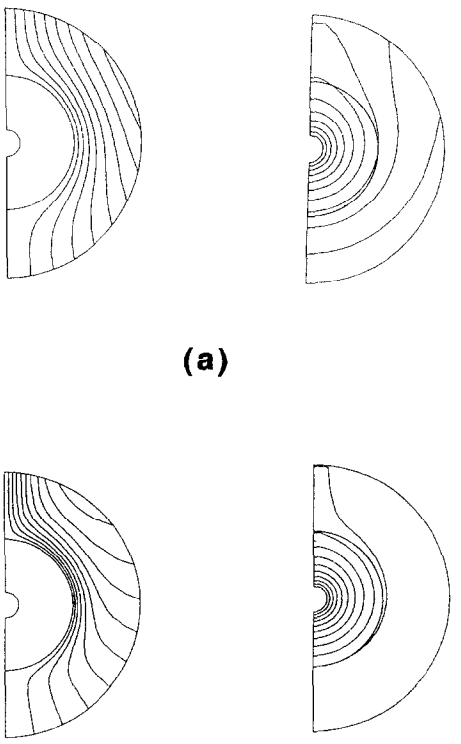

FIG. 2. Streamlines and isotherms for $k = 1$ and $R = 0.2$, (a) $Ra = 20$, $\Delta\psi = 0.5$ and $\Delta\theta = 1$; (b) $Ra = 400$, $\Delta\psi = 2$ and $\Delta\theta = 0.1$.

equation (16) can therefore be replaced by

$$\begin{aligned} &\partial\psi/\partial r = 0, \\ &\theta_f = 0 \quad \text{if} \quad \partial\psi/\partial\phi < 0, \quad \text{at } r = A. \\ &\partial\theta_f/\partial r = 0 \quad \text{if} \quad \partial\psi/\partial\phi > 0 \end{aligned} \tag{26}$$

In order to determine an appropriate finite distance A from a cylinder, we did several calculations varying A from 3 to 15. The results of the average Nusselt number for $k \to \infty$ are given in Table 1 and compared with the analytical solutions by Ingham and Pop (1987). It is seen from the table that $A = 10$ is large enough to produce an accurate numerical result. Next we fixed $A = 10$, and refined the grid network in the porous region from 40×31 to 50×41. The average Nusselt numbers in Table 2 show that the differences between the two are well below 1%.

The partial differential equations (11)–(13) were finite-differenced employing control volume approach and non-uniform grid network as described by Patankar [29]. The total number of the nodal points varied from 1333 (43 in the radial direction and 31 in the angular direction) to 2911 depending upon R (the ratio of the core radius to the cylinder one) and Ra, the Rayleigh number. The convergence of the temperature distribution was monitored at each iteration. The convergence criterion needed for termination of computation was preassigned as

$$\frac{\sum_{i}^{M}\sum_{j}^{N} |\theta_{f_{ij}}^{n+1} - \theta_{f_{ij}}^{n}|}{\sum_{i}^{M}\sum_{j}^{N} \theta_{f_{ij}}^{n+1}} < 10^{-6} \tag{27}$$

where the superscript n denotes the iteration order.

It should be noted that although computations were performed for a large range of values of the parameters k, R and Ra, we present here results only for $k = 0.5$, 1, 4, 20 and ∞; $R = 0.2$, 0.5 and 0.9; $Ra = 10$, 20, 40, 100, 400 and 800. The output has been displayed in terms of streamlines, isotherms, average temperature as well as the average Nusselt numbers.

5. RESULTS AND DISCUSSION

5.1. *Streamline and isotherm pattern*

Detailed streamline and isotherm behavior are presented in Figs. 2–4 for $k = 1$ and 20; $Ra = 20$ and 400. In these plots the results are illustrated for three values of R, namely, $R = 0.2$, 0.5 and 0.9. Each curve in the plots on the left-hand side represents a streamline

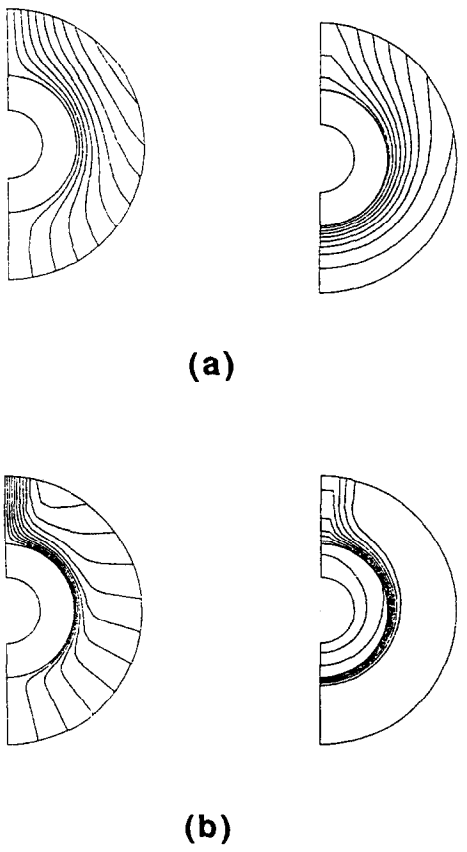

FIG. 3. Streamlines and isotherms for $k = 20$ and $R = 0.5$, (a) $Ra = 20$, $\Delta\psi = 1$ and $\Delta\theta = 0.1$; (b) $Ra = 400$, $\Delta\psi = 5$ and $\Delta\theta = 0.1$.

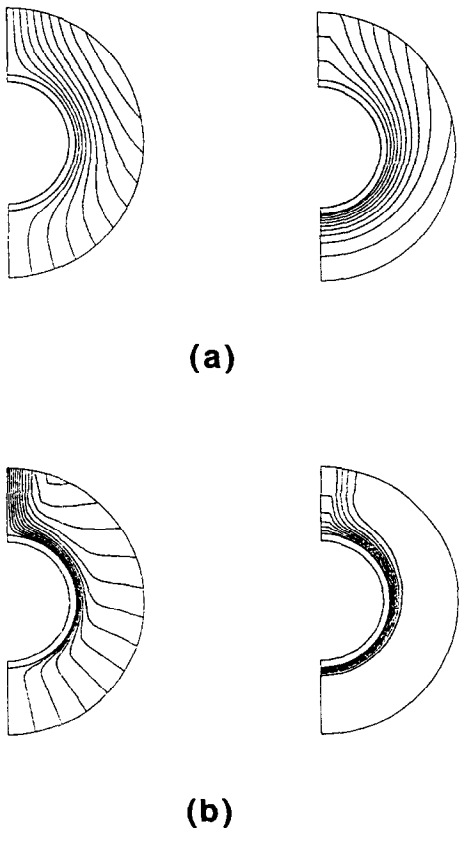

FIG. 4. Streamlines and isotherms for $k = 20$ and $R = 0.9$, (a) $Ra = 20$, $\Delta\psi = 1$ and $\Delta\theta = 0.1$; (b) $Ra = 400$, $\Delta\psi = 5$ and $\Delta\theta = 0.1$.

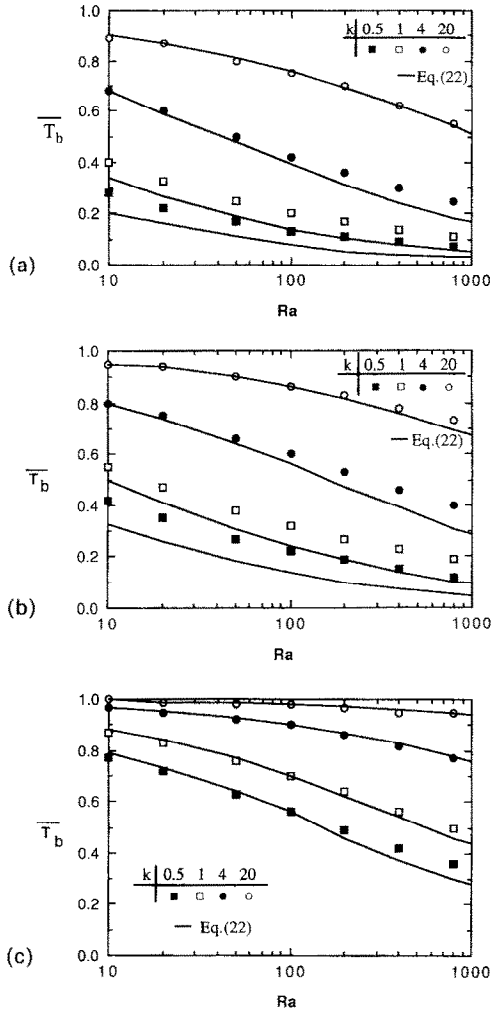

FIG. 5. Variation of the average boundary temperature with Ra, (a) $R = 0.2$; (b) $R = 0.5$; (c) $R = 0.9$.

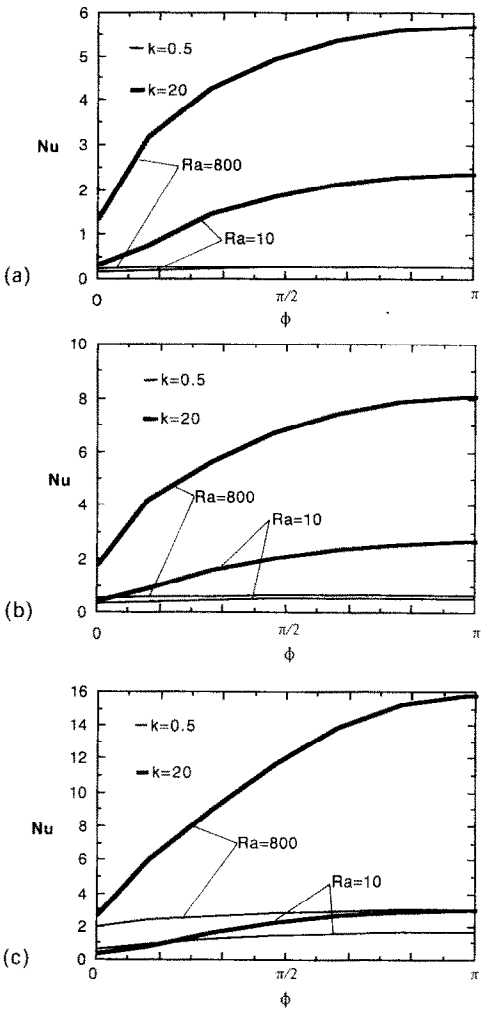

FIG. 6. Variation of the local Nusselt number with ϕ, (a) $R = 0.2$; (b) $R = 0.5$; (c) $R = 0.9$.

while each curve on the right-hand side represents an isothermal line. As is expected, evidence of plume development is found near the top surface of the cylinder. The width of plume decreases as Ra increases and, therefore, the heat transfer activity in the plume region is low; the bottom side of the cylinder dominates the heat transfer in the flow field. This results in great differences between the temperature distribution along the bottom and top symmetry lines. The thermal boundary layer is well developed along the surface of the cylinder and the temperature tends to zero everywhere except in the vicinity of the cylinder and in the plume when Ra is increased. Further, it is seen from these figures that by increasing k the thermal resistance across the cylinder wall becomes weaker and thus the temperature driven force on the fluid porous medium will be stronger. As is evident, however, when comparing the results in Figs. 2(a)–4(a) with those in Figs. 2(b)–4(b), the parameter Ra has a stronger effect on the flow and temperature fields than the parameter k.

Complementary to the previous six figures, Figs. 5–8 depict the effects of the involved parameters in this problem on the temperature and heat transfer coefficients.

5.2. *Temperature distribution*

In Fig. 5 the variation of the average temperature at the solid–fluid interface with respect to Ra for several values of k (as indicated on graphs) and three values of R is shown. The analytical solution represented by equation (22) is also plotted (full lines) for comparison. These figures clearly show a very good agreement between the theoretical and numerical prediction of T_b especially for higher values of k, which is in accord with the discussion on Ra in Section 3. Further, we see that the average temperature is greatly influenced by the conjugated parameter k; it increases as k is increased.

5.3. *Heat transfer coefficients*

Figure 6 shows the distribution of the local Nusselt number along the cylinder surface. The results are

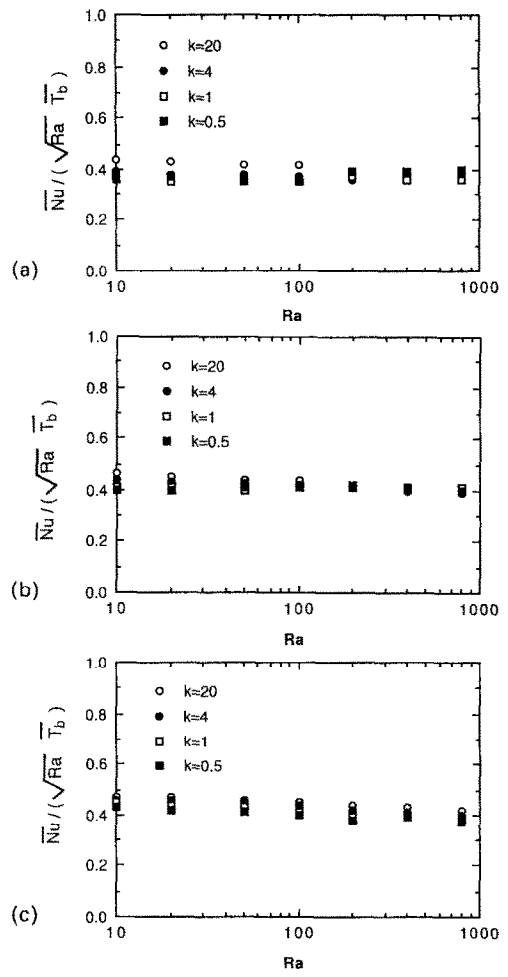

FIG. 7. Variation of $\overline{Nu}/(Ra^{1/2}\,\overline{T_b})$ with Ra, (a) $R = 0.2$; (b) $R = 0.5$; (c) $R = 0.9$.

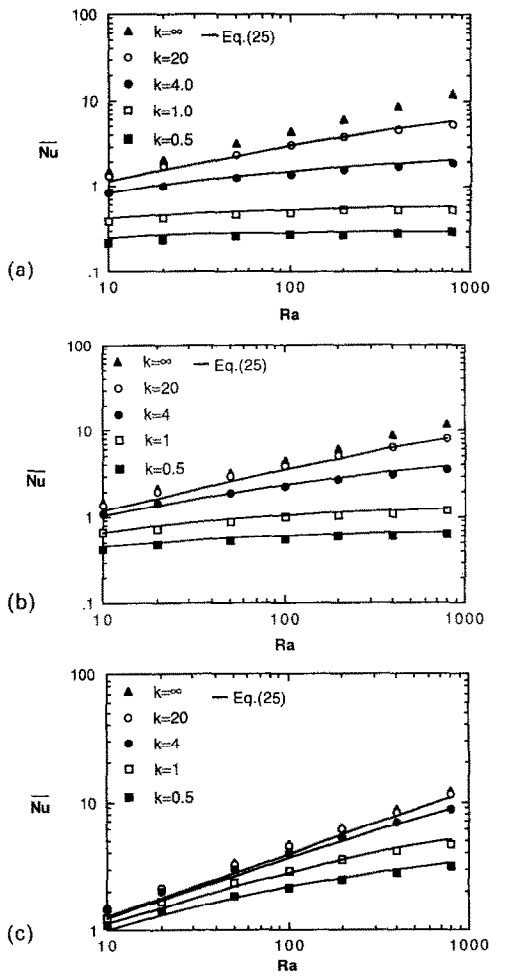

FIG. 8. Variation of the average Nusselt number with Ra, (a) $R = 0.2$; (b) $R = 0.5$; (c) $R = 0.9$.

depicted for $k = 0.5$ and 20; $Ra = 10$ and 800 when $R = 0.2$, 0.5 and 0.9. Again, the remarkable effect of k is clear. As k is increased, the local Nusselt number is increased especially on the bottom side of the cylinder.

The variation of $\overline{Nu}/(Ra^{1/2}\,\overline{T_b})$ with Ra for four values of k and three values of R is illustrated in Fig. 7. As was already noted in Section 3, we see here that this quantity remains constant and has a value of 0.4 ($=\lambda$). This enables us to suggest the analytical formula (25) for the evaluation of the average Nusselt number $\overline{Nu}$. The reasons for this choice are: (i) the simplicity in its structure and (ii) it is a very convenient formula for engineering calculations. On the other hand, it is worth mentioning that the constant $\lambda = 0.4$ is very close to $\overline{Nu}/Ra^{1/2} = 0.444$ reported for the problem of free convection boundary layer about an isothermal vertical plate suspended in a porous medium, see Cheng and Minkowycz [30]. This is consistent with the limiting case of $k \to \infty$ and $Ra \to$ large but finite in equation (23).

In Fig. 8 we have shown the variation of the average Nusselt number with Ra for several values of k and R. The analytical solution (25) has also been displayed here (full lines). Again, the agreement between numeric and approximate solution is very good.

Finally, we notice that the effect of the radius ratio R on the heat transfer results can be studied by comparing the results in Figs. 5–8. It can thus be observed that for the same values of k and Ra, the average temperature and heat transfer coefficients are smaller for smaller values of R ($=0.2$, say) than those for larger values of R ($=0.9$, say). This is so because for smaller R the solid insulation layer is thicker than that for larger R.

6. CONCLUSIONS

This investigation has solved the problem of conjugate free convection from a horizontal circular cylinder with a heated core region immersed in a fluid-saturated porous medium. The geometry considered, means that a vertical symmetry plane exists and the problem is solved only for the vertical half plane. The finite-differential equations formulated in polar coordinates have yielded very accurate results for flow and heat transfer characteristics. In the case of the

boundary layer approximation simple approximate formulae for the average temperature at the surface of the cylinder and average Nusselt number were found, which compare very well with the exact numerical solutions. The authors believe that these formulae are well suited for the problem because of the ease with which they can be handled and accuracy with which the average temperature and the average Nusselt number can be evaluated.

Acknowledgements—The authors gratefully acknowledge a number of constructive comments made by the reviewer.

REFERENCES

1. P. Cheng, Geothermal heat transfer. In *Handbook of Heat Transfer Applications* (Edited by W. M. Rohsenow, J. P. Hartnett and E. N. Ganic), 2nd Edn, Chap. 11. McGraw-Hill, New York (1985).
2. A. Bejan, Convective heat transfer in porous media. In *Handbook of Single-Phase Convective Heat Transfer* (Edited by S. Kakac, R. K. Shah and W. Aung), Chap. 16. Wiley, New York (1987).
3. R. T. Fernandez and V. E. Schrock, Natural convection from cylinders buried in a liquid-saturated porous medium. In *Proc. 7th Int. Heat Transfer Conf.*, Munich, Vol. II, pp. 335–340 (1982).
4. J. H. Merkin, Free convection boundary layers on axisymmetric and two-dimensional bodies of arbitrary shape in a saturated porous medium, *Int. J. Heat Mass Transfer* **22,** 1416–1462 (1979).
5. R. H. Nilson, Natural convective boundary-layer on two-dimensional and axisymmetric surfaces in high *Pr* fluids or in fluid-saturated porous media, *J. Heat Transfer* **103,** 803–807 (1981).
6. D. B. Ingham, J. H. Merkin and I. Pop, The collision of free-convection boundary layers on a horizontal cylinder embedded in a porous medium, *Q. J. Mech. Appl. Math.* **36,** 313–335 (1983).
7. M. Hasan and A. S. Mujumdar, Transpiration-induced buoyancy effect around a horizontal cylinder embedded in a porous medium, *Energy Res.* **9,** 151–163 (1985).
8. D. B. Ingham and I. Pop, Natural convection about a heated horizontal cylinder in a porous medium, *J. Fluid Mech.* **184,** 157–181 (1987).
9. A. Nakayama and H. Koyama, Free convection heat transfer over a nonisothermal body of arbitrary shape embedded in a fluid-saturated porous medium, *J. Heat Transfer* **109,** 125–130 (1987).
10. B. Farouk and H. Shayer, Natural convection around a heated cylinder in a saturated porous medium, *J. Heat Transfer* **110,** 642–648 (1988).
11. V. E. Schrock, R. T. Fernandez and K. Kesavan, Heat transfer from cylinders embedded in a liquid filled porous medium, *Proc. 4th Int. Heat Transfer Conf.*, Paris-Versailles, Vol. VII, CT-3.6 (1970).
12. R. M. Fand, T. E. Steinberger and P. Cheng, Natural convection heat transfer from a horizontal cylinder embedded in a porous medium, *Int. J. Heat Mass Transfer* **29,** 119–133 (1986).
13. T. Sano, Unsteady heat transfer from a circular cylinder immersed in a Darcy flow, *J. Engng Math.* **14,** 177–190 (1980).
14. D. B. Ingham and I. Pop, Free-forced convection from a heated longitudinal horizontal cylinder embedded in a porous medium, *Wärme- und Stoffübertr.* **20,** 283–289 (1986).
15. R. Vasantha, G. Nath and I. Pop, Forced convection along a longitudinal cylinder embedded in a saturated porous medium, *Int. Commun. Heat Mass Transfer* **14,** 639–646 (1987).
16. S. Kimura, Forced convection heat transfer about an elliptic cylinder in a saturated porous medium, *Int. J. Heat Mass Transfer* **31,** 197–199 (1988).
17. S. Kimura, Forced convection heat transfer about a cylinder placed in porous media with longitudinal flows, *Int. J. Heat Fluid Flow* **9,** 83–86 (1988).
18. S. Kimura, Transient forced convection heat transfer from a circular cylinder in a saturated porous medium, *Int. J. Heat Mass Transfer* **32,** 192–195 (1989).
19. I. Pop and P. Cheng, Flow past a circular cylinder embedded in a porous medium based on the Brinkman model, *Int. J. Engng Sci.* (in press).
20. I. Pop, J. K. Sunada, P. Cheng and W. J. Minkowycz, Conjugate free convection from long vertical plate fins embedded in a porous medium at high Rayleigh numbers, *Int. J. Heat Mass Transfer* **28,** 1629–1636 (1985).
21. I. Pop, D. B. Ingham, P. J. Heggs and D. Gardner, Conjugate heat transfer from a downward projecting fin immersed in a porous medium, *Proc. 8th Int. Heat Transfer Conf.*, San Francisco, pp. 2635–2640 (1986).
22. J. Y. Liu and W. J. Minkowycz, The influence of lateral mass flux on conjugate natural convection from a vertical plate fin in a saturated porous medium, *Numer. Heat Transfer* **10,** 507–520 (1986).
23. J. Y. Liu, S. D. Shih and W. J. Minkowycz, Conjugate natural convection about a vertical cylindrical fin with lateral mass flux in a saturated porous medium, *Int. J. Heat Mass Transfer* **30,** 623–630 (1987).
24. A. Nakayama and H. Koyama, Effect of thermal stratification on free convection within porous medium, *J. Thermophys.* **1,** 282–285 (1987).
25. B. Sundén, Conjugated heat transfer from circular cylinders in low Reynolds number flow, *Int. J. Heat Mass Transfer* **23,** 1359–1367 (1980).
26. B. Sundén, Influence of buoyancy forces and thermal conductivity on flow field and heat transfer of circular cylinders at small Reynolds number, *Int. J. Heat Mass Transfer* **26,** 1329–1338 (1983).
27. S. Kimura and I. Pop, Conjugate natural convection between horizontal concentric cylinders filled with a porous medium, *Wärme- und Stoffübertr.* **27,** 85–91 (1992).
28. S. Kimura and I. Pop, Non-Darcian effects on conjugate natural convection between horizontal concentric cylinders filled with a porous medium, *Fluid Dynamics Res.* **7,** 241–254 (1991).
29. S. V. Patankar, *Numerical Heat Transfer and Fluid Flow*. Hemisphere, Washington, DC (1980).
30. P. Cheng and W. J. Minkowycz, Free convection about a vertical flat plate embedded in a porous medium with application to heat transfer from a dike, *J. Geophys. Res.* **82,** 2040–2044 (1977).

CONVECTION NATURELLE CONJUGUEE A PARTIR D'UN CYLINDRE CIRCULAIRE NOYE DANS UN MILIEU POREUX

Résumé—Le but de l'étude est de formuler et de résoudre le problème de la convection naturelle permanente à partir d'un cylindre circulaire horizontal, avec un coeur chauffé, noyé dans un milieu poreux saturé de fluide. Les équations sont résolues numériquement en utilisant une technique de différences finies. Le rapport des conductivités de la paroi du cylindre et du milieu poreux varie de 0,5 à l'infini. Le rapport des rayons intérieur et extérieur du cylindre a les valeurs 0,2, 0,5 et 0,9. Les résultats sont comparés à la solution exacte du cas extrême d'un problème non conjugué. On obtient ainsi des solutions approchées pour la température moyenne de la frontière entre le cylindre et la matrice poreuse et pour le nombre de Nusselt moyen, et les résultats sont confirmés par des calculs numériques. On peut remarquer que cette étude donne des formules compactes pour fournir une information sur la distribution de température et sur le transfert thermique à partir du cylindre, ce qui peut être utile dans beaucoup d'applications en technologie thermique.

KONJUGIERTE FREIE KONVEKTION AN EINEM KREISZYLINDER IN EINEM PORÖSEN MEDIUM

Zusammenfassung—In der vorliegenden Arbeit wird das Problem der stationären freien Konvektion an einem horizontalen Kreiszylinder mit beheiztem Kern, der in ein flüssigkeitsgesättigtes poröses Medium eingebettet ist, formuliert und gelöst. Die Bilanzgleichungen werden mit einem effizienten Finite-Differenzen-Verfahren numerisch gelöst. Der Einfluß unterschiedlicher Eingangsparameter ist in tabellarischer und grafischer Form dargestellt. Das Verhältnis der Wärmeleitfähigkeiten der Zylinderwand und des porösen Mediums wird im Bereich zwischen 0,5 und unendlich variiert. Für das Verhältnis von innerem zu äußerem Zylinderradius wird 0,2; 0,5 und 0,9 gewählt. Die Ergebnisse werden mit der exakten Lösung für den Extremfall eines nicht-konjugierten Problems verglichen. Näherungslösungen für die mittlere Randtemperatur zwischen Zylinder und poröser Matrix und für die mittlere Nusselt-Zahl werden ebenfalls ermittelt. Die Ergebnisse werden von den numerischen Berechnungen bestätigt. Es soll angemerkt werden, daß die vorliegende Analyse komprimierte Formeln liefert, um nützliche Informationen über die Temperaturverteilung und den Wärmetransport an einem Zylinder bereitzustellen, was weitreichende Anwendungen auf dem Gebiet der Wärmetechnik finden kann.

СОПРЯЖЕННАЯ СВОБОДНАЯ КОНВЕКЦИЯ ОТ КРУГОВОГО ЦИЛИНДРА, ПОМЕЩЕННОГО В ПОРИСТУЮ СРЕДУ

Аннотация—Целью настоящего исследования является формулировка и решение задачи стационарной свободной конвекции от горизонтального кругового цилиндра, нагретая центральная часть которого помещена в насыщенную жидкостью пористую среду. Определяющие уравнения решались численно с использованием эффективного метода конечных разностей. Эффекты различных параметров, входящих в задачу, представлены в виде таблиц и графиков. Значения отношения теплопроводностей стенки цилиндра и пористой среды изменялись от 0,5 до бесконечности. Отношение внутреннего и внешнего радиусов цилиндра составляло 0,2; 0,5 и 0,9. Результаты сравнивались с точным решением для экстремального случая несопряженной задачи. Найдены также приближенные решения для средней температуры границы между цилиндром и пористой матрицей, а также для среднего числа Нуссельта, и получено подтверждение результатов численными расчетами. Можно отметить, что настоящий анализ дает компактные формулы для получения полезной информации о распредении температур и теплообмене цилиндра, которые могут широко использоваться для описания различных технологических тепловых процессов.